

# 187 Digital volume correlation of freeze cast aerogel during *in situ* compression using phase contrast synchrotron X-ray micro-CT

S.D. Rawson<sup>1a</sup>, V. Bayram<sup>2</sup>, P. Yang<sup>2</sup>, S. A. McDonald<sup>1</sup>, Y. Guo, J. Xu<sup>2</sup>, T. L. Burnett<sup>1</sup>, S. Barg<sup>2</sup>, P.J. Withers<sup>1</sup>

<sup>1</sup> Henry Royce Institute, School of Materials, University of Manchester, Oxford Road, Manchester, M13 9PL, UK. <sup>2</sup>School of Materials, University of Manchester, Oxford Road, Manchester, M13 9PL, UK.

<sup>a</sup>shelley.rawson@manchester.ac.uk

## Introduction

Freeze casting produces tailorable aerogel structures, which exhibit a highly porous, hierarchical structure of parallel aligned sheets arranged in domains of different angular alignment. Compression of these materials is of particular interest for energy storage applications as a means of obtaining a high packing density of parallel sheets, which is thought to improve capacitive performance so long as an open-pore structure is maintained so not to inhibit ion transport [1, 2]. However, the behaviour of these materials during compression is currently unexplored; further understanding the compression process of aerogels will provide a further mechanism to create the best microstructures, with the aim of achieving improved energy and power density. Traditional imaging modalities, such as scanning electron microscopy (SEM) require cutting to reveal the delicate internal structure, which may cause damage to the aerogel [3]. X-ray micro-computed tomography ( $\mu$ CT) provides an alternative imaging approach, allowing non-destructive 3D imaging and microstructural observations during *in situ* compression. Herein we compare aerogel imaging using SEM and  $\mu$ CT, and use time-lapse tomography along with digital volume correlation (DVC) strain measurements to assess the rearrangement and collapse of the aerogel during compression.

## Methods

Aerogel samples were prepared (3 samples) by suspending exfoliated MXene sheets in de-ionized water (15mg/ml or 30 mg/ml concentration) followed by freeze casting (2.5 °C/min or 5 °C/min) using custom made apparatus (for laboratory of synchrotron  $\mu$ CT imaging respectively). Ice was removed by freeze-drying (FreeZone 4.5L, Labcoanco, USA) leaving the 1x1x1 cm cube of MXene aerogel intact.

To enable SEM imaging of internal features, plasma focussed ion beam (pFIB) milling was used to remove surface material from one aerogel sample (FEI Xe+ plasma source focussed ion beam operated under 30keV and 0.18  $\mu$ A). This was followed by SEM imaging at 5 keV and 86 pA, followed by high resolution laboratory source  $\mu$ CT.

Laboratory source  $\mu$ CT was performed using a Zeiss Versa XRM-520 and XRM scout-and-scan control system (V 1.1.5707.17179, Zeiss, Oberkochen) during tomography of the pFIB milled sample at high resolution, and also for low resolution time lapse imaging of one sample during *in situ* compression. Imaging was performed at an energy of 60 keV or 70 keV, power of 5 W or 6 W, taking 3001 or 2001 projections with 75 s or 4 s exposure time for high and low resolution imaging respectively through 360° of rotation. The source to sample distance was 43mm for both, the sample to detector distance was 73 mm or 103 mm, and a 4x or 0.39x objective was used for high and low resolution imaging respectively, providing some phase contrast, which enhances the detection of the aerogel sheets. High resolution imaging provided a voxel size of 1.25  $\mu$ m and a 2.5 mm field of view and low resolution provided a voxel size of 10.00  $\mu$ m with the whole sample within the field of view.

Synchrotron X-ray source tomography was performed at the European Synchrotron Radiation Facility using the ID15A beamline to perform time-lapse imaging of one sample during *in situ* compression. Imaging was performed at 40 keV energy and 100 ms exposure time, taking 1500 projections through 180° of sample rotation. Sample to detector distance was 100 mm to allow some in-line phase contrast (PC) in order to enhance visibility of the aerogel sheets. This provided a voxel size of 3.2  $\mu$ m and a 4.4 mm field of view.

*In situ* compression was performed using custom equipment, applying 0.5 mm or 1 mm displacement steps to a maximum of 50% or 20% compression, for synchrotron and laboratory X-ray source imaging respectively.  $\mu$ CT was performed prior to compression and after each loading step. A filtered back projection algorithm was used to reconstruct tomography data followed by data visualisation and analysis using Avizo (version 9.7; FEI Visualisation Sciences Group) and DaVis (version 8.2.2; LaVision) for digital volume correlation to perform analysis of strain and deformation throughout the 3D structure.

## Results and Discussion

Aerogel sheets observed by SEM imaging and using laboratory source PC  $\mu$ CT at high resolution, demonstrating that PC  $\mu$ CT is suitable for the observation of aerogel microstructure. Additionally, CT data revealed that aerogel structure adjacent to the surface differs from that within the bulk of the material, suggesting that surface imaging using SEM is unsuitable.  $\mu$ CT did not require sample cutting to reveal internal features, which is necessary with SEM and could damage the delicate structure. Whilst we have demonstrated that sample cutting and subsequent SEM imaging is achievable using FIB milling, this was extremely time consuming, provided a very limited field of view compared with  $\mu$ CT imaging, and was not compatible with *in situ* compression for subsequent DVC. The thickness of the aerogel sheets appears to be much greater from PC  $\mu$ CT imaging compared with sheet thickness as observed with SEM due to the large voxel size and use of PC, therefore a limitation of PC  $\mu$ CT at the settings used herein is that it cannot be used to reliably determine aerogel sheet thickness.

Laboratory source  $\mu$ CT data of the whole sample under compression was analysed by DVC. Results demonstrated non-uniform compression throughout the aerogel; whilst the sheets within some regions become compacted, those in other regions do not. Observations using high resolution synchrotron source  $\mu$ CT imaging suggest that the non-uniform compaction is due to orientation of the sheets of the aerogel sheets with respect to the loading direction prior to compression. Sheets within domains which are parallel to the loading direction did not rotate as force was applied (fig 1 a and b), whereas sheets in unaligned domains rotated towards being perpendicular to the applied load during compression, and their plane spacing also decreased (fig 1 c and d).

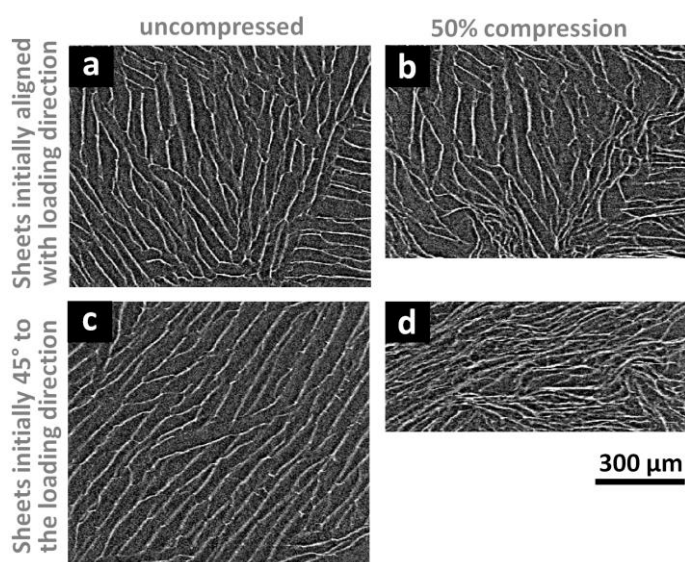


Fig 1, synchrotron  $\mu$ CT data of the aerogel, showing regions of the sample initially aligned with the loading direction, or at  $45^\circ$  to the loading direction in the uncompressed sample (a and c) and following 50% compressed (b and d).

## Conclusions

Both laboratory and synchrotron source  $\mu$ CT imaging enable reliable observation of the microstructural arrangement of aerogel sheets and domains, and DVC can be performed following *in situ* compression. DVC demonstrated heterogeneous compression of the aerogel microstructure. We hypothesise that electrochemical performance is affected by this non-uniform compression by blocking pores in over-compressed domains.

## References

- [1] H. Cao, X. Zhou, W. Deng, Z. Liu. *A compressible and hierarchical porous graphene/Co composite aerogel for lithium-ion batteries with high gravimetric/volumetric capacity*. Journal of Materials Chemistry A, Vol. 4(16) (2016) p. 6021-6028.
- [2] J.-Y. Hong, B. M. Bak, J. J. Wie, J. Kong, H. S. Park. *Reversibly compressible, highly elastic and durable graphene aerogel for energy storage devices under limiting conditions*. Advanced Functional Materials. Vol. 25 (2014) p. 1053-1062.
- [3] A. Ghafar. *Synchrotron microtomography reveals the fine three-dimensional porosity of composite polysaccharide aerogels*. Materials. Vol. 10(8) (2017) p. 871.